Geomorphology 449 (2024) 109031

Contents lists available at ScienceDirect

Geomorphology

journal homepage: www.journals.elsevier.com/geomorphology

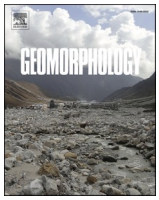

Sediment fluxes within salt marsh tidal creek systems in the Yangtze Estuary

Jianwei Sun [a,b], Bram van Prooijen [b], Xianye Wang [a,*], Zhonghao Zhao [a], Qing He [a], Zhengbing Wang [b,c]

[a] State Key Laboratory of Estuarine and Coastal Research, East China Normal University, 500 Dongchuan Road, Shanghai 200241, China
[b] Faculty of Civil Engineering and Geosciences, Delft University of Technology, Stevinweg 1, Delft 2628 CN, the Netherlands
[c] Deltares, 177, Delft 2600 MH, the Netherlands

ARTICLE INFO

Keywords:
Sediment flux
Marsh creek systems
Sediment availability

ABSTRACT

Creeks are essential for salt marshes by conveying water and sediment through this geomorphic system. In this paper, we investigate the mechanisms that determine the residual sediment flux using measurements conducted in tidal creeks in salt marshes of the Yangtze Estuary. A main creek and a secondary creek were studied to explore whether the mechanisms determining residual sediment fluxes through the main creek differ from those in the secondary creek. Measurements in creeks were carried out over 5 years, spanning different months. Sediment import was found during most tides, both in the main creek and the secondary creek, implying that creeks in Chongming generally function as a conveyor belt of sediment into the marsh. However, sediment export can occur during certain overbank tides. When comparing the role of creeks in drainage and sediment delivery, the main creek functions more in delivering sediment while the secondary creek primarily serves as a drainage conduit. To better understand the mechanisms behind sediment fluxes, the residual sediment flux was compared with the residual discharge and the sediment differential (differences in sediment concentration between flood and ebb). Overbank tides generally lead to a net outward discharge as more water from saltmarshes can be concentrated into the marsh creek during ebb tides. This net outward discharge tends to export more sediment during ebb tides. However, due to the sediment abundance during the flood phase in the turbid environment, sediment import can be expected even with the residual export of water. Export of sediment was only found for the few tides with a net outward discharge and a small positive sediment concentration differential. Large negative sediment differentials (larger averaged suspended sediment concentration during ebb tides) have not been observed because the sediment supply during ebb is limited. This paper unravels how the sediment differential and residual discharge contribute to the residual sediment flux, providing a better understanding of sediment dynamics in marsh creek systems.

1. Introduction

Salt marshes are multi-functional: they attenuate waves and protect shorelines during storms (Leonardi et al., 2016), provide habitats for a range of species, including migratory birds (Hughes, 2004), and sequester carbon (Lockwood and Drakeford, 2021). Therefore, the preservation of salt marshes is a key component for coastal management. However, one of the issues is whether they can keep pace with accelerating sea-level rise. Sufficient sediment supply is needed, not only at the edge of the salt marsh but also deeper into the marsh. Saltmarsh creeks are perceived as dynamic conduits for transporting sediment. Yet, their role in sediment transport is intricate, as they can either import or export sediment. Consequently, understanding net sediment fluxes in marsh creeks is essential for the preservation of salt marshes.

Net sediment transport is determined by both the tidal asymmetry and the difference in sediment concentration between flood and ebb tides. Boon (1975) found that asymmetry in flow velocity could result in sediment transport towards salt marshes. Tidal asymmetry in salt marshes is caused by the difference in friction and depth between creeks and the vegetated marsh (French and Stoddart, 1992). These mechanisms have been further explored and reviewed in Fagherazzi et al. (2013). They also highlighted the effect of sediment resuspension on the

* Corresponding author.
E-mail address: xywang@sklec.ecnu.edu.cn (X. Wang).

https://doi.org/10.1016/j.geomorph.2023.109031
Received 3 June 2023; Received in revised form 17 December 2023; Accepted 17 December 2023
Available online 4 January 2024

adjacent mud flats, leading to high sediment concentrations during flood stages. Coleman et al. (2020) and Nowacki and Ganju (2019) show that the net sediment flux through creeks depends on the asymmetry in sediment concentration: if the concentration during flood is higher than during ebb, a net inward flux is found, and vice versa. The difference in sediment concentration between flood and ebb could be a consequence of local resuspension, or due to erosion/deposition elsewhere. The quantitative contribution of the asymmetry in flow and in sediment concentration to net sediment fluxes remains unclear.

Various factors can play a role in the net import/export of sediment through salt marsh creeks. For example, large river discharges or strong winds can bring more water and more sediment into creeks (Green and Hancock, 2012; Nowacki et al., 2019; Wang et al., 2020). Seasonal variations in bioturbation (Leonard et al., 1995) and drag by vegetation (Lacy et al., 2020) can influence sediment transport processes within salt marshes. In addition, inundation events are crucial for the net sediment flux towards salt marshes (Fagherazzi et al., 2012). When a salt marsh is not inundated, the flow is confined within the creek, and the velocity is relatively low (Pieterse et al., 2016). When a salt marsh is inundated, overbank tides occur, leading to higher velocities in marsh creeks. High flow velocities in the creek may erode sediment that was deposited in previous tides (Xie et al., 2018a). Sediment transport is influenced by these factors through their impacts on the asymmetries in flow and in sediment concentration.

The interplay between flow and sediment is complex. An often-made assumption is that the sediment concentration scales with the hydrodynamic forcing. For example, Fagherazzi and Priestas (2010) and Fagherazzi et al. (2013) show that the concentration during flood scales with the wave height on the mudflat just in front of the marsh and with the velocity during the ebb stage. Such an assumption is only valid if there is sufficient sediment available. Davidson-Arnott et al. (2002) found that the interaction between flow and sediment is not always scaled, as suspended sediment concentration (SSC) remained consistent with changing hydrodynamics. This possibly indicates that less sediment becomes available for erosion. In that case, erosion is supply-limited. Supply limitation plays a crucial role in sediment concentration and thus affects sediment fluxes. The occurrence of supply limitation in marsh creeks within a turbid system will also be investigated.

The role of marsh creeks in sediment transport may vary under different conditions. In this paper, we explore the mechanisms behind sediment fluxes further to explain how, when, and why sediment is transported towards or out of the salt marsh. We measured flow velocities, depths, and sediment concentrations in creeks in the marsh of Chongming Island, China. We test the statement of Nowacki and Ganju (2019) within the salt marsh tidal creek systems in a turbid estuary: the sediment concentration differential indicates the direction of residual sediment fluxes. Furthermore, we explore the influence of net water discharge on the direction and magnitude of residual sediment fluxes. In this way, we aim to reveal a better understanding of sediment dynamics, especially net sediment fluxes, in marsh creeks.

2. Regional setting

Chongming Island is located in the Yangtze Estuary, China (Fig. 1a and b). It has been expanding eastwards at rates of 10 m/year over past centuries (Yang et al., 2001). Due to accelerated sea-level rise and the decreasing fluvial sediment supply since 2008the accretion rate of the eastern shoreline has decreased, with a rate of 2.81 km^2/year from 1985 dropping to a rate of 0.15 km^2/year after 2008 (Wang et al., 2022). Chongming Island is regarded a turbid area with an annual averaged tidal range of approximately 2.6 m (Ding and Hu, 2020). In Chongming Island, the wet season is in summer (June–September), while the dry season is in winter (November–February). The main creek is defined as the widest creek close to the mudflat, while the secondary creek is defined as the tributary that is directly connected with the main creek.

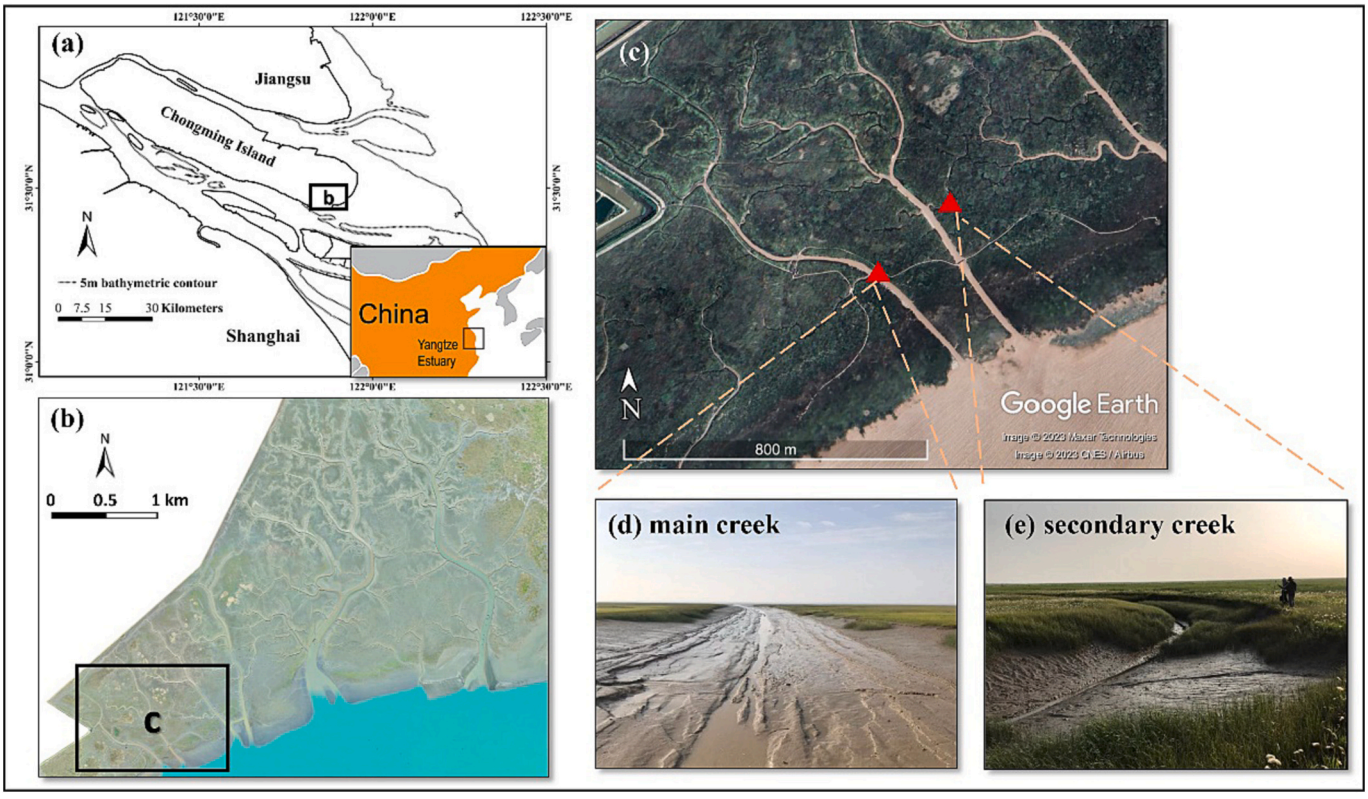

Fig. 1. (a) Map of the Yangtze Estuary; (b) Drone image of salt marshes in Eastern Chongming Island; (c) Google Earth map of the study area showing locations of measurement sites. Source aerial imagery: Google Earth. (red triangles represent the measuring locations); (d) A photo of the main creek and (e) the secondary creek.

3. Method

3.1. Experiment set up

Two sites were selected: one in a main creek and one in a secondary creek (Fig. 1c). To cover this seasonal variation of river discharges and also the state of marshes, we measured the dynamics in different months. Ideally, the measurements would last for a full year to cover all seasonal variations. Due to operational restrictions, the measurements were carried out in the months March, April, May (at the start of the wet season) and in September (at the end of the wet season) in various years. Measurements in the main creek were conducted in April and September (2015). These data sets have been partly presented already in Wang et al. (2020). Here we utilized these data to investigate the mechanisms behind sediment fluxes in the main creek, while Wang et al. (2020) focuses more on local morphological changes in the creek. Measurements in the secondary creek were carried out in late May (2018) and March (2019). Although the measurements of the main creek and the secondary creek were not conducted simultaneously, we believe that we can use these as a comparison because the hydraulic characteristics of the secondary creek are similar for these years. The monthly average discharge for these four months at Datong station was 2.43×10^4 m^3/s, 2.84×10^4 m^3/s, 2.99×10^4 m^3/s and $3.06 \times /10^4$ m^3/s, respectively (data source is River Sediment Bulletin of China in http://www.cjh.com.cn/). Effects of local waves were not significant within our measurements. During the measurements of the main creek, the average wave heights were below 0.08 m in April and below 0.04 m in September (Wang et al., 2020). In addition, the impacts of waves were limited due to the vegetation in the secondary creek. The measuring location in the main creek is approximately 500 m upstream of the salt marsh edge. The depth of the main creek is approximately 2 m. The creek is drained during low tide. The bed level of the main creek is fairly uniform over the width of about 30 m (see Fig. 1d). The second measurement location is at the thalweg of a vegetated meandering secondary creek (see Fig. 1e). The width of the secondary creek is approximately 4 m and the depth is approximately 1.5 m. The distinction between underbank flow and overbank flow is defined at water depths of 1.45 m and 1.4 m for the main creek and the secondary creek, respectively. Morphological changes were not measured in the secondary creek.

Flow velocities and water depths were measured with an ADCP (1.0 MHz or 2.0 MHz Aquadopp Profiler, Nortek AS, Norway) or an ADV (Acoustic Doppler velocimeters, Nortek AS, Norway), see Table 1. Turbidity was measured with OBS (OBS-3 A, D&A Instrument Company, Washington, USA). The ADVs were installed 55 cm above the bed in the main creek, facing downwards. The measuring point is thereby approximately 40 cm above the bed. The OBSes in the main creek were deployed 15 cm above the bed. The ADCPs were placed 10 cm above the bed in the secondary creek, facing upwards. The transmitters of the OBSes were positioned 10 cm above the bed as well. The burst intervals and burst periods of ADV or ADCP are indicated in Table 1. The OBSes were synced with the ADV/ADCP. More details of the measuring period are provided in Table 1.

Table 1
An overview of the instruments set up.

Location	Instrument	Measuring period	Burst intervals (s)	Burst period (s)
Main creek	ADV + OBS	01.04.2015–11.04.2015	600	60
Main creek	ADV + OBS	16.09.2015–22.09.2015	300	30
Secondary creek	ADCP + OBS	26.05.2018–02.06.2018	300	60
Secondary creek	ADCP + OBS	18.03.2019–26.03.2019	300	60

3.2. Data processing

The velocity data was de-spiked using the approach proposed in Zhu (2017): threshold values of the amplitude and correlation were used to remove invalid data. Velocities were transformed into a coordinate system with a stream-wise (along-creek) and transverse component. ADCP results were averaged over the depth. As ADVs in our measurements only collected data at about 40 cm above the bed, we assumed that the velocities measured by ADVs can represent the depth-averaged velocities. The turbidity data with water levels higher than the velocity sensor and with valid velocity data were taken as reliable data. A few outliers of velocities and turbidity signals were removed manually.

Calibration of the OBSes was carried out in the laboratory, using in-situ sediment samples. Following the procedure described in Hoitink and Hoekstra (2005), the calibration curves are added as supplementary material.

Translating our measurements into discharges and sediment fluxes requires integration over the cross-section. Flow velocity profiles are averaged over the depth and the sediment concentration is assumed uniform over the depth. Similar to Green and Hancock (2012) and van Weerdenburg et al. (2021), the cumulative discharge (Q_a) and cumulative sediment flux (F_a) per unit width are obtained from the data sets of the instantaneous velocity, water depth, and SSC:

$$Q_a = \sum_0^t v(t) \bullet D(t) \bullet \Delta t \tag{1}$$

$$F_a = \sum_0^t v(t) \bullet D(t) \bullet c(t) \bullet \Delta t \tag{2}$$

where v is the velocity in creek direction, D is the water depth and c is the suspended sediment concentration.

The results of the accumulated discharge and sediment flux per unit width are shown, for a better comparison between the main creek and secondary creek. Multiplying with the width would result in too much difference, due to the much larger width of the main creek.

In order to explore the mechanisms of residual sediment fluxes, we use a similar method to obtain the specific residual discharge (ΔQ) and residual sediment flux (ΔF) per unit width:

$$\Delta Q_i = Q_a\left(t_{i,end}\right) - Q_a\left(t_{i,begin}\right) \tag{3}$$

$$\Delta F_i = F_a\left(t_{i,end}\right) - F_a\left(t_{i,begin}\right) \tag{4}$$

where $t_{i,begin}$ is the start time of a tidal cycle i and $t_{i,end}$ is the end of tidal cycle i. The tidal cycles are easily distinguished, as the creeks fall dry. Therefore, residual discharge (ΔQ) and residual sediment flux (ΔF) for each tidal cycle can be determined. Positive values indicate a net import of water or sediment, and negative values indicate a net export of water or sediment.

The sediment differential between flood and ebb (ΔC) is defined as the difference between the mean flood concentration and the mean ebb concentration (Nowacki and Ganju, 2019):

$$\Delta C = \frac{1}{n_{flood}} \sum_{i=1}^{n_{flood}} c_i - \frac{1}{n_{ebb}} \sum_{i=1}^{n_{ebb}} c_i \tag{5}$$

where n_{flood} and n_{ebb} represent the number of SSC data points for the flood tide and ebb tide, respectively. A positive value thereby indicates that the averaged flood concentration is higher than the averaged ebb concentration, and vice versa.

4. Results

4.1. Main creek

A distinct spring-neap tidal cycle can be recognized (Figs. 2a and 3a). During neap tide, the flow was restricted to the creek (the water depths

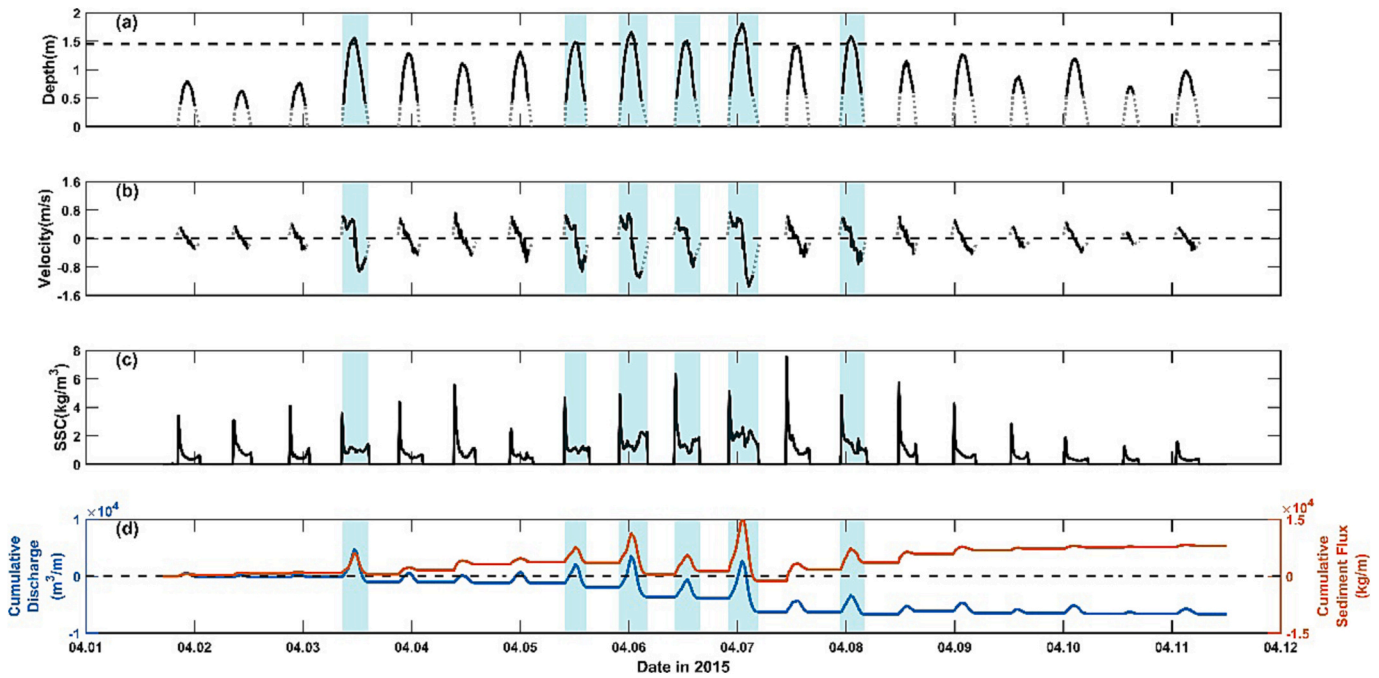

Fig. 2. Time series of (a) water depth (The dashed line represents the creek depth), (b) velocity (flood velocity is positive), (c) Suspended sediment concentration, and (d) cumulative discharge and sediment flux (into the creek is positive) in the main creek in April 2015. The grey dotted data of water depths and velocities are interpolated by linear methods to synchronize them with the SSC data quantities. The overbank tides were highlighted in blue.

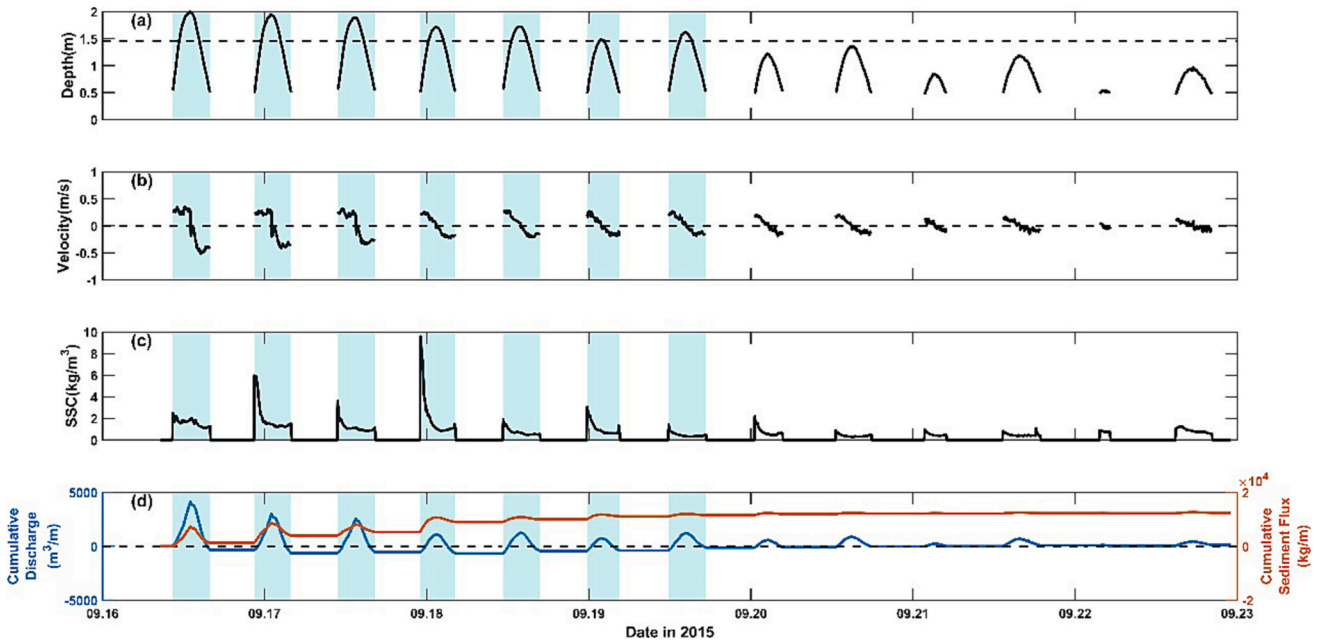

Fig. 3. Time series of (a) water depth (The dashed line represents the creek depth), (b) velocity (flood velocity is positive), (c) Suspended sediment concentration, and (d) cumulative discharge and sediment flux (into the creek is positive) in the main creek in September 2015. The overbank tides were highlighted in blue.

are <1.45 m). During spring tide, the water level exceeded the marsh level, and overbank flow occurred. The flow velocities were higher during overbank flow (Figs. 2b and 3b), due to the larger tidal volume when the bank was exceeded. In addition to the spring-neap cycle, daily inequity was found. The ebb velocities during overbank tides were higher in April than in September.

An evident peak in SSC appeared at the beginning of each tidal cycle, i.e., when the creek was flooded (Figs. 2c and 3c). The SSC in the main creek can reach 7.5 kg/m^3 in April and 9.5 kg/m^3 in September. The largest SSC did not occur during the tides with the largest water depths and velocities (e.g., T11 in April and T1 in September). The highest peak in SSC for each tide did not occur at the same time as the peak velocity. For some tides, a clear peak in SSC during ebb can be found just before drying. These peaks were however lower than flood peaks.

During underbank tides with shallow water, flow velocities were low, leading to negligible import/export of water. During overbank tides with high water levels, there was a clear export of water as more water from the marsh would be concentrated into the marsh creek during ebb

tides. The creeks functioned as a drain. In April, we saw a weak sediment import during underbank tides but sediment export during overbank tides (Fig. 2d), whereas in September, an import of sediment was observed with the net export of water during overbank tides (Fig. 3d). The net import of sediment depended on the substantial sediment supply during flood tides. Cumulative sediment fluxes over both periods were positive, i.e. sediment import.

4.2. Secondary creek

Typical spring and neap tides can also be observed in the secondary creek (Figs. 4a and 5a). There was a similar pattern of hydrodynamics between March and May in the secondary creek. During underbank tides, similar peaks of velocity can be observed between flood and ebb tides. While a distinct peak of velocity appeared during overbank ebb tides (Figs. 4b and 5b).

The SSC in the secondary creek showed contrasting patterns between the two months. In March, a recognizable peak can be found at the beginning of each tidal cycle, and for some tides, a smaller peak in SSC during ebb was found (Fig. 4c). In late May, the maximum SSC was higher at the beginning of the flood during underbank tides. However, compared with the peak at the beginning of flood, a much larger peak in SSC during ebb can be seen during overbank tides (Fig. 5c). Note that the magnitude of SSC in May was smaller. The maximum SSC reached approximately 1.6 kg/m^3 in March but was $<$0.6 kg/m^3 in May. Thus, comparing with the SSC in the main creek, the SSC in the secondary creek was much smaller, which results in the weak role of the secondary creek in sediment transport.

The cumulative discharges were negative during both measurement periods, indicating the export of water. This is because more water from the marsh would converge into tributaries during overbank tides. The secondary creek serves more as a conduit for drainage. However, the secondary creek functioned differently between two months. In March, the secondary creek imported more sediment during overbank tides (Fig. 4d). In May, sediment was transported out of the secondary creek during overbank tides (Fig. 5d). Though a small amount of sediment was transported into the secondary creek during underbank tides, the cumulative sediment flux was still negative in May, indicating that more sediment was exported back to the main creek from the secondary creek. The difference in sediment fluxes between two months is determined by the variation in SSC patterns. In March, a flood SSC peak can be observed during overbank tides. This flood peak in SSC can lead to more sediment import during flood tides. While in May, an ebb SSC peak occurred during overbank tides, leading to more export of sediment during ebb tides.

4.3. Residual sediment fluxes

The direction of residual sediment fluxes is determined by the difference of sediment fluxes between flood and ebb tides. When there is more sediment transport during the flood tide than during the ebb tide, it results in sediment import within that tidal cycle, and conversely, sediment export occurs when the sediment transport during the ebb tide surpasses the sediment transport during the flood tide (Fig. 6a). The dashed line indicates the conditions for which the sediment flux during flood equals the sediment flux during ebb. The majority of the markers is below this line, indicating larger fluxes during flood than during ebb, implying a net import per tidal cycle. We furthermore see that the import is larger for larger sediment concentration differentials (larger markers), which aligns well with Nowacki and Ganju (2019): the direction of net sediment flux can be inferred from the SSC differential. For some tidal cycles, however, we do see an export of sediment for a large tidal range (warm colors) and a small sediment concentration differential (small markers). Those are observed for the secondary creek (triangles) and the main creek (circles).

To gain deeper insights into how the sediment differential and the net discharge influence the residual sediment flux, we plotted the residual sediment flux (ΔF) as a function of the sediment differential (ΔC) and the net discharge (ΔQ). Four quadrants can be identified in Fig. 6b, based on the signs of ΔC and ΔQ. No tide is found with ΔQ $>$0 and ΔC $<$0 (case 4) during our measurement campaigns.

A closed water balance would imply that ΔQ equals zero. However, based on our data sets, we found that the net discharge is not always zero. Both positive and negative values for ΔQ were found. A positive net discharge indicates that water stays in the creek system (for both underbank and overbank tides) or in the marsh (for overbank tides). A

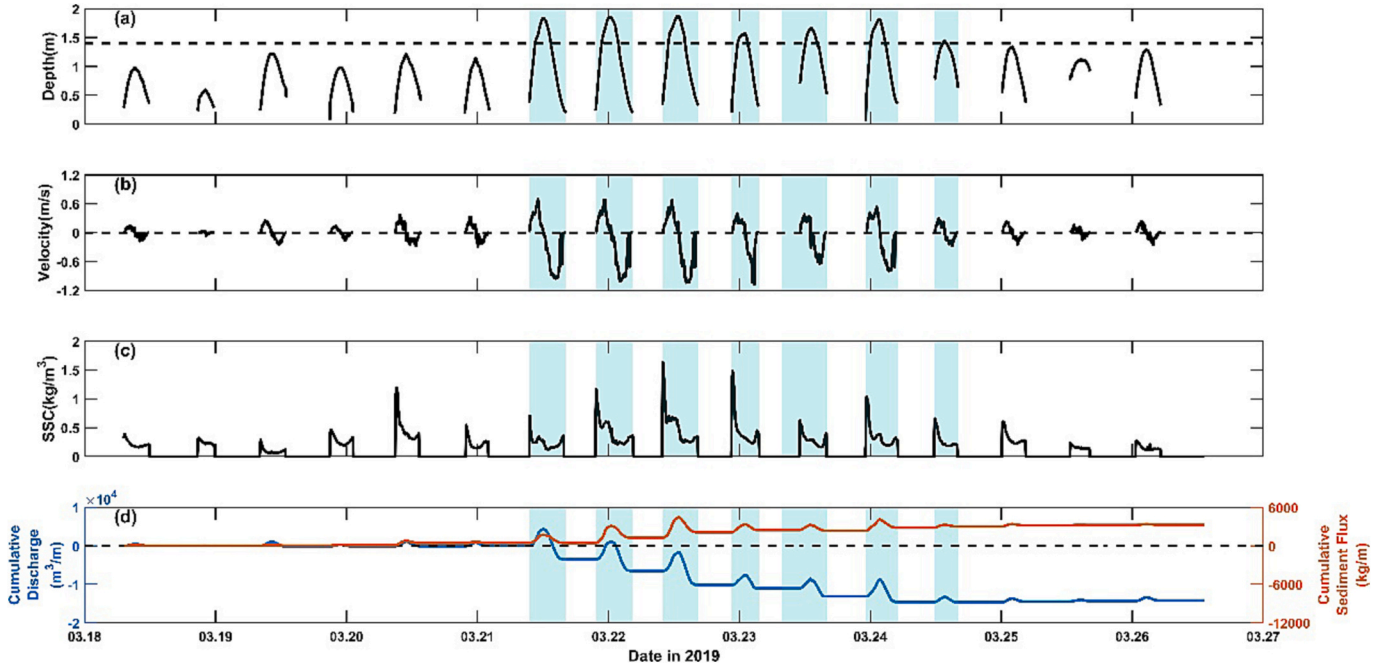

Fig. 4. Time series of (a) water depth (The dashed line represents the creek depth), (b) velocity (flood velocity is positive), (c) Suspended sediment concentration, and (d) cumulative discharge and sediment flux (into the creek is positive) in the secondary creek in March 2019. The overbank tides were highlighted in blue.

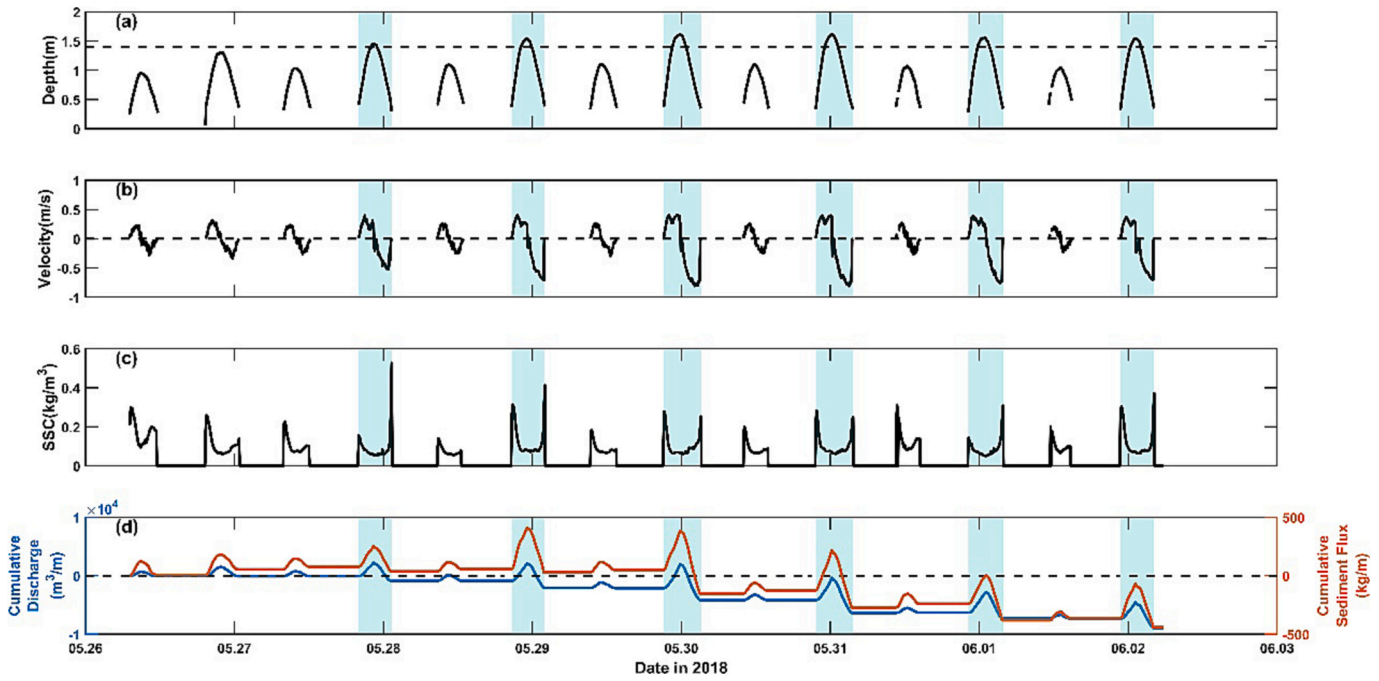

Fig. 5. Time series of (a) water depth (The dashed line represents the creek depth), (b) velocity (flood velocity is positive), (c) Suspended sediment concentration, and (d) cumulative discharge and sediment flux (into the creek is positive) in the secondary creek in May 2018. The overbank tides were highlighted in blue.

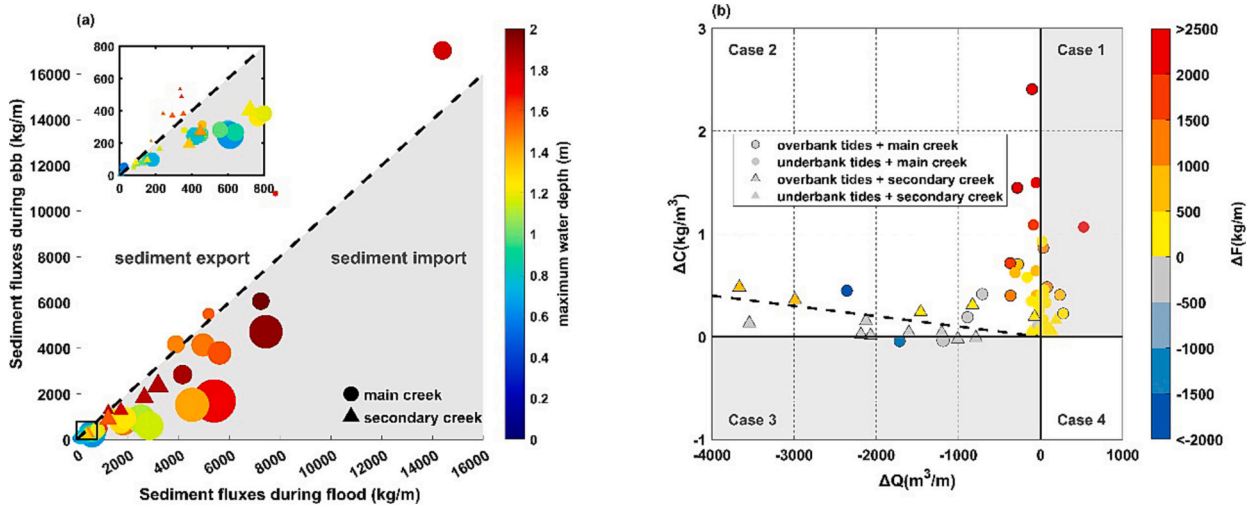

Fig. 6. (a)Residual sediment fluxes between flood and ebb tides. Circles are the data in the main creek, and triangles are the data in the secondary creek. The size of the circles and triangles represent the absolute value of SSC differential between flood and ebb tides. The colour indicates the maximum water depth during that tidal cycle; (b)Relationship among ΔC (differential of SSC between flood and ebb), ΔQ (residual discharge) and ΔF (residual sediment flux) for each tide cycle. Points with edges represent overbank tides. Positive ΔQ and ΔF indicate onshore net transport of water and sediment, respectively. Positive ΔC indicates larger SSC during the flood tide than during the ebb tide.

negative value indicates that water from somewhere else (e.g., from the marsh edge in case of overbank flow) is drained through the creek.

In the first quadrant (case 1), ΔQ and ΔC are both positive, representing the onshore net import of water and higher SSC during flood than during ebb for these tide cycles, respectively. In this case, sediment fluxes are as expected all positive. Only small positive residual discharges can be found in this quadrant. The small positive residual discharge during underbank tides is likely a consequence of groundwater recharge and the substantial drainage basin of creeks, which provides the potential for water to be kept in the tributaries. As for the positive residual discharge during overbank tides, there are some possibilities for explaining smaller amounts of water were transported in the marsh creek during ebb tides than during flood tides: (i) groundwater played a role; (ii) part of the water stayed in the tributaries; (iii) the overflowing water from the creek was exported to other creek systems nearby.

In the second quadrant (case 2), where $\Delta Q < 0$ and $\Delta C > 0$, the water is exported, and the mean SSC during flood is larger than during ebb. In this quadrant, negative residual sediment fluxes are found mainly during overbank tides, and these fluxes are mainly <500 kg per unit width per tide. A line is drawn to indicate a distinction between positive and negative sediment fluxes. This line suggests that negative net sediment fluxes ($\Delta F < 0$) can be found for situations with higher concentrations during flood than during ebb ($\Delta C > 0$) as long as the net discharge is

substantially negative ($\Delta Q < 0$). Four points with large negative sediment flux are found in the main creek, and three of them occur during overbank tides. For other tides, the residual sediment fluxes are positive. The tides with a large value of ΔF have large positive ΔC (> 0.5 kg/m^3).

Two trends are found between ΔQ and ΔC: (i) Substantial export of water (large negative values for ΔQ) is accompanied by small values of ΔC. In those cases, the higher ebb flow can mobilize sufficient sediment to balance the generally higher SSC during flood. (ii) High concentration differentials are found for small values of ΔQ. The ebb flow is not strong enough to generate sufficiently high concentrations. This is likely a characteristic for high-turbid systems like the Yangtze Estuary. A large ΔF is found for large ΔC and low ΔQ.

Only three tides fall in the third quadrant (case 3), with $\Delta Q < 0$ and $\Delta C < 0$. These three tides all occur during overbank tides. Two are found in the secondary creek and one is found in the main creek. Sediment export can be observed during these three tides, as it could be expected for tides with a net outflow of water and higher concentrations during ebb than during flood.

To sum up, overbank tides can result in negative ΔQ, as a substantial amount of water from the marsh can be concentrated into the marsh creek during the ebb tide. This asymmetry in flow tends to export sediment due to the more dominant ebb flow. However, in a turbid system, such as Chongming, a high flood peak of SSC can be expected, leading to a positive ΔC. This asymmetry in sediment concentration can sometimes counteract the tendency to export sediment caused by the asymmetry in flow during overbank tides, which can lead to a net import of sediment. The dotted line in Fig. 6b indicates varying degrees of the asymmetry in SSC required to counteract the asymmetry in flow. A larger net discharge in marsh creeks, a larger sediment differential is required to ensure the role of marsh creeks in importing sediment.

5. Discussions

5.1. Determination of sediment fluxes from point measurements

Determining the discharge and sediment flux is complicated due to the non-uniformity of the flow velocity and sediment concentration over the depth and width, as well as the variation of the creek width over the depth. Furthermore, sinuosity of the channel leads to non-uniformity in the velocity and concentration distribution over the cross-section. Such non-uniformities can lead to non-linear effects on sediment fluxes. Limited by point measurements, we cannot account for the non-uniformity. Based on point measurements, the instantaneous sediment flux can be estimated by the geometry (water depth D and width W) and the flow velocity u and sediment concentration c in the measurement point: $F = \int_{dA}(uc)dA = \alpha uDWc$. The coefficient α represents the effects of all non-uniformities in the cross-section. In case $\alpha = 1$, the estimated sediment flux equals the real sediment flux. In case $\alpha =$ constant, the value of the net sediment flux scales linearly with the real net sediment flux. This implies that the sign of the estimated sediment flux is correct for a constant α. In reality, α will vary over time, as the velocity and concentration distribution over the cross-section vary over time. In studies where sediment fluxes were estimated based on point measurements, the (implicit) assumption of $\alpha = 1$ is often made (Green and Hancock, 2012; Colosimo et al., 2020, and Andersen and Pejrup, 2001), based on the assumption of close to uniform distributions of the sediment concentration. This is true if the mixing is sufficiently strong. An additional potential limitation of this approach is that high turbidity during extremely shallow water was not captured due to the blanking distance of the field instruments. High SSC may occur during periods of very shallow water (Zhang et al., 2016). However, water depths are also very small during these periods. These shallow water periods are therefore considered to have little effects on our conclusions for the residual sediment fluxes.

In addition, we also ignore the width variation over the tidal cycle for the sediment flux per unit width, which may lead to additional errors. In order to discuss the errors in the sediment flux due to the variation of width, we compute the fluxes based on the topography data of the main creek in 2016 from Xie et al. (2018a). The maximum depth and width of the main creek are about 2 m and 30 m, respectively. The sediment flux can be affected by the shape of the creek as the width is not uniform over the height (Fig. 7a and b). We calculated the sediment fluxes with and without considering the creek shape, see Fig. 7c. The sediment flux considering the creek shape is obtained by the cross-section, velocity, and sediment concentration. A width of 17 m turns out to be the representative width. For that width, the accumulated sediment flux based on a constant width is equal to the accumulated sediment flux with a varying creek width. The average difference between two methods is 18 %. Although the values for α might not be constant, the results from Fig. 7 indicate that they are sufficiently accurate to draw conclusions about the role of the creeks.

Measurements in the main creek and in the secondary creek were conducted at the relatively straight section of the creek. In addition, we focused on the residual sediment flux at along-creek direction. Therefore, tidal meanders were not considered in our work. However, due to the complex of dynamics in meandering creeks, more sediment can be transported towards the inner/convex bank because of the secondary flow (Finotello et al., 2019; Wang et al., 2020).

5.2. Availability of sediment and supply-limitation

The sediment fluxes are affected by the availability of sediment. SSC and velocities are not always correlated. High velocities can sometimes carry only a small amount of sediment due to limited sediment supply. Conversely, high SSC values can sometimes be observed for low velocities when the sediment supply is high. To investigate the sediment carrying capacity, we analyse the relationship between the sediment concentration and the flow velocity.

We first consider the concentration and flow velocity in the main creek (Fig. 8a). The concentration is plotted on a logarithmic scale to cover the large range. For visualization, a trend line is included in the plot to highlight different sediment carrying capacity. The trend lines are different for September and April. For the same velocity, higher concentrations are found in September than for April. This would imply that the sediment is easier to erode in September or that the sediment has a smaller settling velocity in September. A difference is also found between flood and ebb. The slopes of the trend lines during flood are higher than during ebb. This implies that more sediment is carried during flood than during ebb, but this sediment did not completely return during ebb again. This would indicate that the settling and scour lag processes (van Straaten and Kuenen, 1958) are potential mechanisms for net sediment transport.

The relation between the concentration and flow velocity in the secondary creek (Fig. 8b) is substantially different from the one in the main creek. The concentrations during ebb are hardly influenced by the local flow velocity. They are also low compared to the flood stage and compared to the concentrations in the main creek. These low concentrations indicate that there was limited sediment supply, as the tidal current was capable enough to carry more sediment but less sediment was in the water column. The difference between ebb and flood indicates that during flood much more sediment was available, likely from the main creek or the upstream of the secondary creek. The measurements in March and May show the same pattern, but higher concentrations are found during the March campaign. These differences between months could have two causes. On the one hand, the difference in vegetation between months can have impacts on SSC (Nardin et al., 2020): the density of vegetation is higher in May than in March. The state of vegetation can affect local erosion, deposition, and also the transport of sediment (Brückner et al., 2020). On the other hand, external forces, e.g., strong precipitation or winds, could lead to more sediment import from mud flats to creeks (Gomes et al., 2013; Green and Coco, 2007;

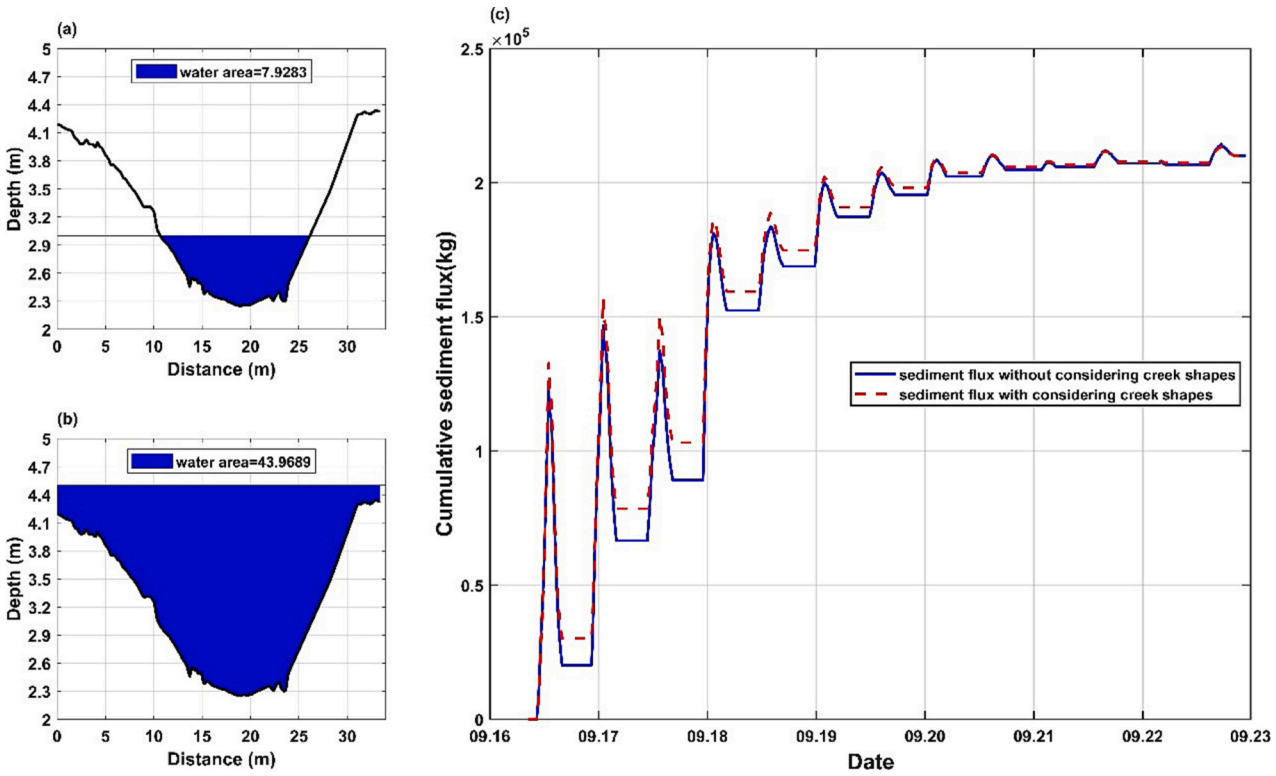

Fig. 7. The comparison of sediment fluxes between two methods: (a)An example of the water area during underbank tide (tidal elevation = 3 m); (b) An example of the water area during overbank tide (tidal elevation = 4.5 m); (c) cumulative sediment flux based on two methods (the blue solid line represents the result using the method in this work; the red dash line represents the result with considering the real creek shape).

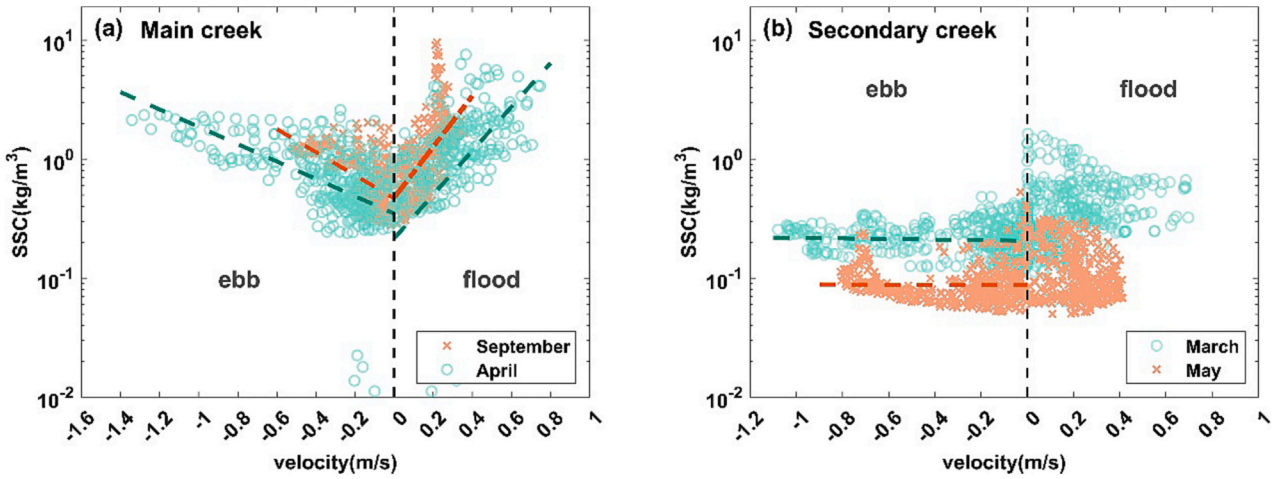

Fig. 8. Different sediment availability in creek systems in different months: (a)the relationship between velocity and SSC in the main creek in two months; (b)the relationship between velocity and SSC in the secondary creek in two months. Positive velocities represent flood velocities and negative velocities represent ebb velocities.

Lacy et al., 2018). Both causes can have significant impacts on sediment availability in creeks. The source of the measured high sediment concentrations, however, needs further investigation.

As stated by Ganju et al. (2015), the system is steered by the availability of erodible material. Even in a turbid system like the Yangtze Estuary, we see in the secondary creek, a lack of sediment is limiting the import of sediment. The transport capacity of the flow is not the limiting factor. The key is that sediment beds can develop such a strength that erosion is not possible anymore, even for velocities up to 1 m/s.

5.3. *Role of creeks in sediment flux within the marsh*

To classify the role of creeks in Chongming in delivering water and sediment, the residual flux of water and sediment in saltmarsh creeks are conceptualized in Fig. 9 for: (i) two types of creeks (a main and a secondary creek); (ii) underbank tides and the overbank tides; (iii) differences in sediment availability.

Overbank tides can lead to negative net discharge in creek systems as more water from the marsh can converge into creeks. This has a positive impact on the survival of marsh vegetation (Morzaria-Luna et al., 2004; Schepers et al., 2017), since creeks result in faster drainage of the marsh

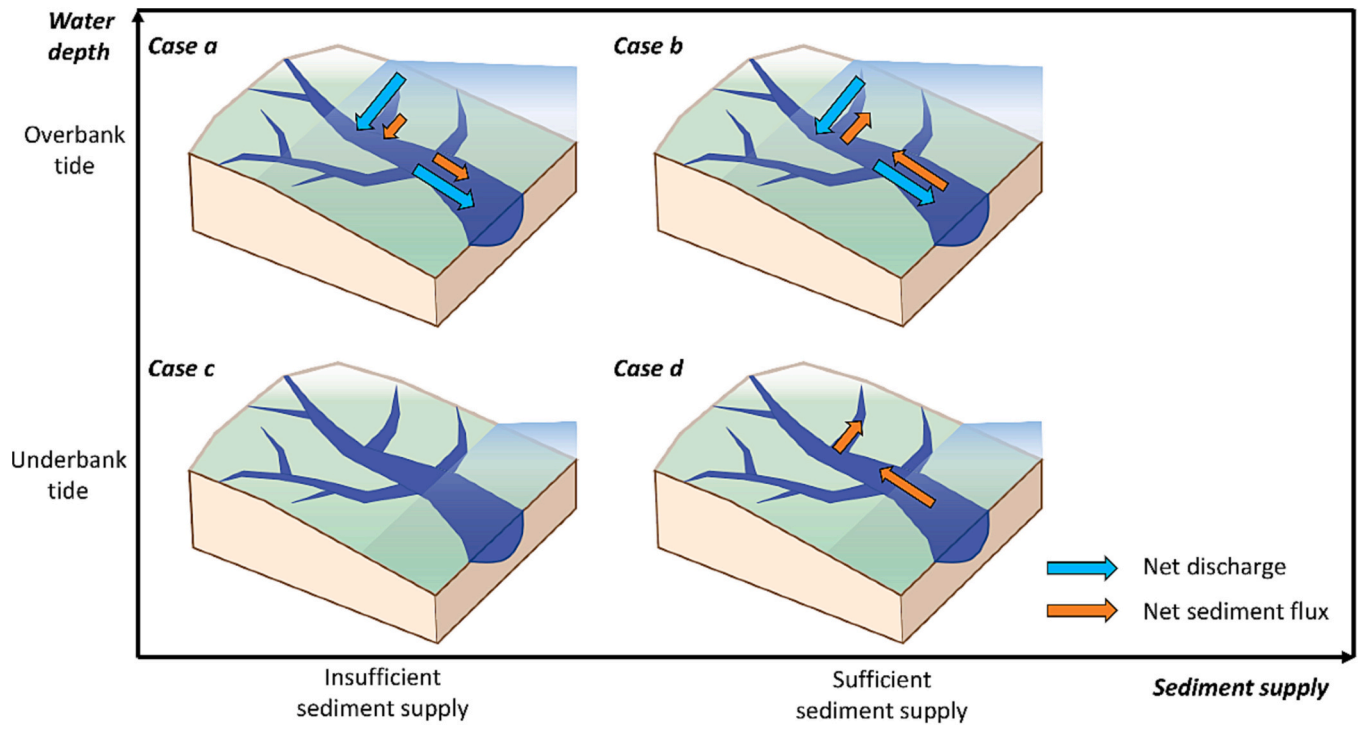

Fig. 9. Residual discharge and sediment flux in saltmarsh creek systems under different conditions of overbank tides and underbank tides with different availability of sediment supply in Chongming. Arrows indicate the net discharge (blue) and the net sediment flux (yellow).

as indicated by van Belzen et al. (2017). Whether this net outward discharge also results in a net export of sediment depends tidal asymmetry processes and sediment availability. Tidal asymmetry in combination with sufficient sediment availability on the mudflats generally results in a net import of sediment (Fig. 9: case b). In those cases, the sediment concentration during flood is sufficiently high and ebb flow is not strong enough to bring sediment back again. These conditions are, for example, described in Rinaldo et al. (1999). Only if the sediment availability is sufficiently small (to bring sediment inward during flood) and if the outflowing velocities are sufficiently high (due to the extra discharge), sediment can be exported via the creek out of the salt marsh system. We measured such conditions (small concentration differential and relatively high net discharge) for several tides, as indicated in Fig. 6b: the tides below the dashed line. Note that the sediment fluxes are small for those tides. These conditions are indicated in Fig. 9: case a).

During underbank tides without more water being concentrated from the marsh to the creek during ebb tide, the discharge is approximately zero (Fig. 9: case c and case d), indicating a water balance. Without sufficient sediment supply, the role of creeks in sediment delivery can be negligible (Fig. 9: case c). However, due to the turbid environment in Chongming, sufficient sediment supply can be expected, even during underbank tides. Consequently, both the main creek and the secondary creek keep importing sediment during underbank tides (Fig. 9: case d). The cumulative sediment import during underbank tides can balance or even surpass the sediment export that occurs during overbank tides, e.g., in April (Fig. 2d). Therefore, the main creek in Chongming generally imports sediment.

Whether there is a net import/export of sediment to the marsh depends on the occurrence of the conditions as sketched in Fig. 9. Waves, which frequently occur in summer in Chongming, can bring more sediment from mudflats to marshes via creeks by increasing the sediment supply (Ladd et al., 2019; Willemsen et al., 2022). Consequently, main creeks in Chongming function more as conduits for importing sediment under wave impacts (Fig. 9: case b and d). However, as the vegetation in the secondary creek can grow in summer, which can reduce the sediment supply (Xu et al., 2022), the secondary creeks in Chongming are expected to serve as channels for drainage rather than sediment transport (Fig. 9: case a and c). Furthermore, under the condition of sea-level rise and a lack of sediment supply, the creeks are likely to export sediment from the marsh system (as illustrated in Fig. 9: case a), which may increase the vulnerability of salt marsh systems to the impacts of climate change.

When comparing the role of creeks in drainage and sediment delivery, we found that the main creek in Chongming primarily serves as a conduit for importing sediment, whereas the secondary creek in Chongming primarily functions as a conduit for drainage. Since the main creek functions more as a conduit for importing sediment to the marsh system in Chongming, we roughly estimate the contribution of the main creek to the vertical accretion of marshes, to give more insights into the role of creeks in delivering sediment. The salt marsh in Chongming has been deposited vertically with an accretion rate of 31 mm/year to 150 mm/year since 2005 (Yang et al., 2020; Xie et al., 2018b). The area of the watershed covering the measuring creek system is around 400 m $\times$ 1200 m. Extrapolating the measurement period to a full year, results in a yearly flux of 4.02×10^6 kg. The dry density of sediment is estimated as 1330 kg/m^3 (Yuan et al., 2020). Therefore, the accretion rate via creeks would be 6.3 mm/year, indicating that creeks can contribute potentially 4 % - 20 % to the vertical accretion of the marsh. Considering the sea-level rise rate of 4.0 mm/year in the Yangtze Estuary (Yang et al., 2020), the role of creeks in contributing to the vertical accretion of marshes in the face of accelerated sea-level rise is significant in Chongming. Furthermore, it should be noted that substantial storm events were not captured during our measurement campaigns. Storm events can provide more sediment to the marsh (Turner et al., 2006, 2007), through creeks and marsh edges. The sediment import induced by storms is determined by the duration and magnitude of storm surges (Castagno et al., 2018). Longer measurements in marsh creeks and also at the marsh edge are required for a more accurate and robust quantification of the role of creeks in the development of marshes.

6. Conclusions

The direction and magnitude of the residual sediment flux are determined by the relative importance of the asymmetry in flow and in sediment concentration. We confirmed the statement of Nowacki and Ganju (2019) that the sediment differential is key for the sediment flux, especially in a turbid inter-tidal environment, like Chongming Island in the Yangtze Estuary. Substantial net export of water via creeks can mainly be found during overbank tides. This asymmetry in flow tends to export sediment with the net discharge. While due to the turbid environment, a high SSC peak during the flood phase can be normally expected, leading to a net sediment import during most tidal cycles. A weak sediment export can be observed during some overbank tides when the sediment differential is not evident. Therefore, the abundance of sediment during flood tides is essential for the import of sediment. Creeks function more as conduits for sediment import due to this asymmetry in sediment concentration.

Our findings unravel the mechanisms behind sediment fluxes, highlighting the importance of sediment availability in delivering sediment via creeks. However, the source of the measured sediment needs further investigation to advance the understanding of the transport regime in creek systems.

CRediT authorship contribution statement

Jianwei Sun: Conceptualization, Investigation, Methodology, Visualization, Writing – original draft. **Bram van Prooijen:** Funding acquisition, Methodology, Supervision, Writing – review & editing. **Xianye Wang:** Conceptualization, Data curation, Funding acquisition, Project administration, Supervision, Writing – review & editing. **Zhonghao Zhao:** Data curation, Investigation, Software. **Qing He:** Funding acquisition, Project administration, Supervision. **Zhengbing Wang:** Funding acquisition, Methodology, Supervision, Writing – review & editing.

Declaration of competing interest

The authors declare that they have no known competing financial interests or personal relationships that could have appeared to influence the work reported in this paper.

Data availability

Data will be made available on request.

Acknowledgments

This study is conducted in the framework of the project "Coping with deltas in transition" within the Programme of Strategic Scientific Alliances between China and the Netherlands (PSA), financed by the Chinese Ministry of Science and Technology (MOST) and the Royal Netherlands Academy of Arts and Sciences (KNAW) (No. 2016YFE0133700). The support from Projects of Natural Science Foundation of China (NSFC) (U2040216, 42276217), Shanghai Science and Technology Committee (Nos. 22dz1202700, 21DZ1201803, 21DZ1201700, 21230750600, 20DZ1204701), Chongming Dongtan Birds National Natural Reserve, Shanghai (CMDT-JC202301), City University Cooperation Project (SXHZ-2022-02-10), and China Scholarship Council (CSC) are also acknowledged.

This article has been partially grammar checked by ChatGPT, an OpenAI language model based in San Francisco, CA, USA.

Appendix A. Appendix

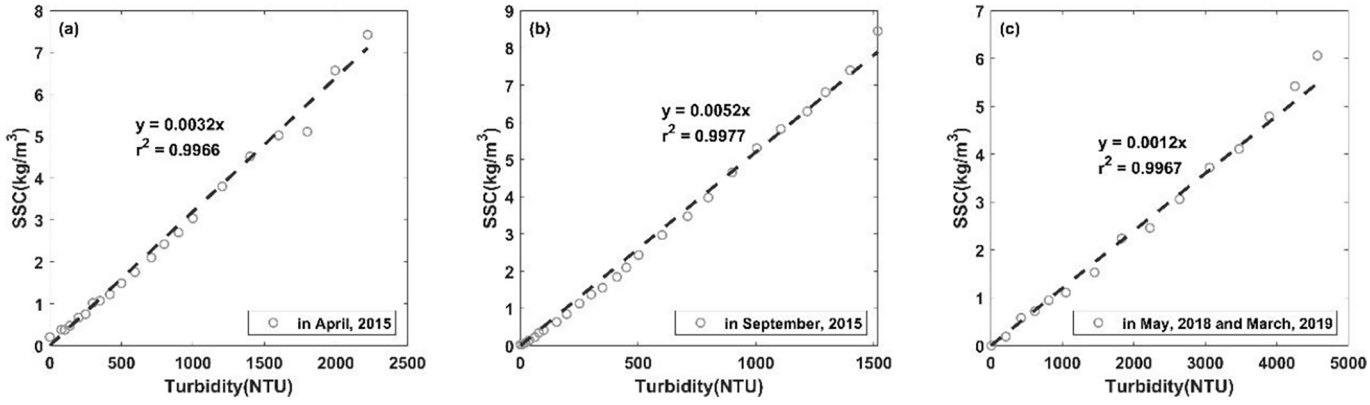

Fig. A.1. Sediment calibration curves of the optical backscatter signal with SSC data in (a) the main creek in April 2015, (b) the main creek in September 2015, and (c) the secondary creek in May 2018 and March 2019.

References

Andersen, T.J., Pejrup, M., 2001. Suspended sediment transport on a temperate, microtidal mudflat, the Danish Wadden Sea. Mar. Geol. 173 (1), 69–85. https://doi.org/10.1016/S0025-3227(00)00164-X.

van Belzen, J., van de Koppel, J., Kirwan, M.L., van der Wal, D., Herman, P.M.J., Dakos, V., Kéfi, S., Scheffer, M., Guntenspergen, G.R., Bouma, T.J., 2017. Vegetation recovery in tidal marshes reveals critical slowing down under increased inundation. Nat. Commun. 8 (1) https://doi.org/10.1038/ncomms15811. Article 1.

Boon, J.D., III., 1975. Tidal discharge asymmetry in a salt marsh drainage system1,2. Limnol. Oceanogr. 20 (1), 71–80. https://doi.org/10.4319/lo.1975.20.1.0071.

Brückner, M.Z.M., Braat, L., Schwarz, C., Kleinhans, M.G., 2020. What came first, mud or biostabilizers? Elucidating interacting effects in a coupled model of mud, saltmarsh, microphytobenthos, and estuarine morphology. Water Resour. Res. 56 (9), e2019WR026945 https://doi.org/10.1029/2019WR026945.

Castagno, K.A., Jiménez-Robles, A.M., Donnelly, J.P., Wiberg, P.L., Fenster, M.S., Fagherazzi, S., 2018. Intense storms increase the stability of tidal bays. Geophys. Res. Lett. 45 (11), 5491–5500. https://doi.org/10.1029/2018GL078208.

Coleman, D.J., Ganju, N.K., Kirwan, M.L., 2020. Sediment delivery to a tidal marsh platform is minimized by source decoupling and flux convergence. J. Geophys. Res. Earth 125 (8), e2020JF005558. https://doi.org/10.1029/2020JF005558.

Colosimo, I., de Vet, P.L.M., van Maren, D.S., Reniers, A.J.H.M., Winterwerp, J.C., van Prooijen, B.C., 2020. The impact of wind on flow and sediment transport over intertidal flats. Journal of Marine Science and Engineering 8 (11). https://doi.org/10.3390/jmse8110910. Article 11.

Davidson-Arnott, R.G.D., van Proosdij, D., Ollerhead, J., Schostak, L., 2002. Hydrodynamics and sedimentation in salt marshes: examples from a macrotidal

marsh, Bay of Fundy. Geomorphology 48 (1), 209–231. https://doi.org/10.1016/S0169-555X(02)00182-4.
Ding, L., Hu, J., 2020. Influence of the salinity intrusion on island water source safety: a case study of the Chongming Island, China. In: Estuaries and Coastal Zones in Times of Global Change. Springer, pp. 47–58. https://doi.org/10.1007/978-981-15-2081-5_4.
Fagherazzi, S., Priestas, A.M., 2010. Sediments and water fluxes in a muddy coastline: Interplay between waves and tidal channel hydrodynamics. Earth Surf. Process. Landf. 35 (3), 284–293. https://doi.org/10.1002/esp.1909.
Fagherazzi, S., Kirwan, M.L., Mudd, S.M., Guntenspergen, G.R., Temmerman, S., D'Alpaos, A., van de Koppel, J., Rybczyk, J.M., Reyes, E., Craft, C., Clough, J., 2012. Numerical models of salt marsh evolution: Ecological, geomorphic, and climatic factors. Rev. Geophys. 50 (1) https://doi.org/10.1029/2011RG000359.
Fagherazzi, S., Wiberg, P.L., Temmerman, S., Struyf, E., Zhao, Y., Raymond, P.A., 2013. Fluxes of water, sediments, and biogeochemical compounds in salt marshes. Ecol. Process. 2 (1), 3. https://doi.org/10.1186/2192-1709-2-3.
Finotello, A., Canestrelli, A., Carniello, L., Ghinassi, M., D'Alpaos, A., 2019. Tidal flow asymmetry and discharge of lateral tributaries drive the evolution of a microtidal meander in the Venice Lagoon (Italy). J. Geophys. Res. Earth 124 (12), 3043–3066. https://doi.org/10.1029/2019JF005193.
French, J.R., Stoddart, D.R., 1992. Hydrodynamics of salt marsh creek systems: Implications for marsh morphological development and material exchange. Earth Surf. Process. Landf. 17 (3), 235–252. https://doi.org/10.1002/esp.3290170304.
Ganju, N.K., Kirwan, M.L., Dickhudt, P.J., Guntenspergen, G.R., Cahoon, D.R., Kroeger, K.D., 2015. Sediment transport-based metrics of wetland stability. Geophys. Res. Lett. 42 (19), 7992–8000. https://doi.org/10.1002/2015GL065980.
Gomes, V.J.C., Freitas, P.T.A., Asp, N.E., 2013. Dynamics and seasonality of the middle sector of a macrotidal estuary. J. Coast. Res. 65 (10065), 1140–1145. https://doi.org/10.2112/SI65-193.1.
Green, M.O., Coco, G., 2007. Sediment transport on an estuarine intertidal flat: Measurements and conceptual model of waves, rainfall and exchanges with a tidal creek. Estuar. Coast. Shelf Sci. 72 (4), 553–569. https://doi.org/10.1016/j.ecss.2006.11.006.
Green, M.O., Hancock, N.J., 2012. Sediment transport through a tidal creek. Estuar. Coast. Shelf Sci. 109, 116–132. https://doi.org/10.1016/j.ecss.2012.05.030.
Hoitink, A.J.F., Hoekstra, P., 2005. Observations of suspended sediment from ADCP and OBS measurements in a mud-dominated environment. Coast. Eng. 52 (2), 103–118. https://doi.org/10.1016/j.coastaleng.2004.09.005.
Hughes, R.G., 2004. Climate change and loss of saltmarshes: Consequences for birds. Ibis 146 (s1), 21–28. https://doi.org/10.1111/j.1474-919X.2004.00324.x.
Lacy, J.R., Ferner, M.C., Callaway, J.C., 2018. The influence of neap–spring tidal variation and wave energy on sediment flux in salt marsh tidal creeks. Earth Surf. Process. Landf. 43 (11), 2384–2396. https://doi.org/10.1002/esp.4401.
Lacy, J.R., Foster-Martinez, M.R., Allen, R.M., Ferner, M.C., Callaway, J.C., 2020. Seasonal variation in sediment delivery across the bay-marsh interface of an estuarine salt marsh. J. Geophys. Res. Oceans 125 (1), e2019JC015268. https://doi.org/10.1029/2019JC015268.
Ladd, C.J.T., Duggan-Edwards, M.F., Bouma, T.J., Pagès, J.F., Skov, M.W., 2019. Sediment supply explains long-term and large-scale patterns in salt marsh lateral expansion and erosion. Geophys. Res. Lett. 46 (20), 11178–11187. https://doi.org/10.1029/2019GL083315.
Leonard, L.A., Hine, A.C., Luther, M.E., 1995. Surficial sediment transport and deposition processes in a Juncus roemerianus marsh, West-Central Florida. J. Coast. Res. 11 (2), 322–336.
Leonardi, N., Ganju, N.K., Fagherazzi, S., 2016. A linear relationship between wave power and erosion determines salt-marsh resilience to violent storms and hurricanes. Proc. Natl. Acad. Sci. 113 (1), 64–68. https://doi.org/10.1073/pnas.1510095112.
Lockwood, B., Drakeford, B.M., 2021. The value of carbon sequestration by saltmarsh in Chichester Harbour, United Kingdom. J. Environ. Econ. Policy 10 (3), 278–292. https://doi.org/10.1080/21606544.2020.1868345.
Morzaria-Luna, L., Callaway, J.C., Sullivan, G., Zedler, J.B., 2004. Relationship between topographic heterogeneity and vegetation patterns in a Californian salt marsh. J. Veg. Sci. 15 (4), 523–530. https://doi.org/10.1111/j.1654-1103.2004.tb02291.x.
Nardin, W., Lera, S., Nienhuis, J., 2020. Effect of offshore waves and vegetation on the sediment budget in the Virginia Coast Reserve (VA). Earth Surf. Process. Landf. 45 (12), 3055–3068. https://doi.org/10.1002/esp.4951.
Nowacki, D.J., Ganju, N.K., 2019. Simple metrics predict salt-marsh sediment fluxes. Geophys. Res. Lett. 46 (21), 12250–12257. https://doi.org/10.1029/2019GL083819.
Nowacki, D.J., Ogston, A.S., Nittrouer, C.A., Fricke, A.T., Asp, N.E., Souza Filho, P.W.M., 2019. Seasonal, tidal, and geomorphic controls on sediment export to Amazon River tidal floodplains. Earth Surf. Process. Landf. 44 (9), 1846–1859. https://doi.org/10.1002/esp.4616.
Pieterse, A., Puleo, J.A., McKenna, T.E., 2016. Hydrodynamics and sediment suspension in shallow tidal channels intersecting a tidal flat. Cont. Shelf Res. 119, 40–55. https://doi.org/10.1016/j.csr.2016.03.012.
Rinaldo, A., Fagherazzi, S., Lanzoni, S., Marani, M., Dietrich, W.E., 1999. Tidal networks: 3. Landscape-forming discharges and studies in empirical geomorphic relationships. Water Resour. Res. 35 (12), 3919–3929. https://doi.org/10.1029/1999WR900238.
Schepers, L., Kirwan, M., Guntenspergen, G., Temmerman, S., 2017. Spatio-temporal development of vegetation die-off in a submerging coastal marsh. Limnol. Oceanogr. 62 (1), 137–150. https://doi.org/10.1002/lno.10381.
van Straaten, L.M.J.U., Kuenen, Ph.H., 1958. Tidal action as a cause of clay accumulation. J. Sediment. Res. 28 (4), 406–413. https://doi.org/10.1306/74D70826-2B21-11D7-8648000102C1865D.
Turner, R.E., Baustian, J.J., Swenson, E.M., Spicer, J.S., 2006. Wetland sedimentation from hurricanes Katrina and Rita. Science 314 (5798), 449–452. https://doi.org/10.1126/science.1129116.
Turner, R.E., Swenson, E.M., Milan, C.S., Lee, J.M., 2007. Hurricane signals in salt marsh sediments: Inorganic sources and soil volume. Limnol. Oceanogr. 52 (3), 1231–1238. https://doi.org/10.4319/lo.2007.52.3.1231.
Wang, H., Xu, D., Zhang, D., Pu, Y., Luan, Z., 2022. Shoreline dynamics of Chongming Island and driving factor analysis based on landsat images. Remote Sens. 14 (14) https://doi.org/10.3390/rs14143305. Article 14.
Wang, X., Sun, J., Zhao, Z., 2020. Effects of river discharge and tidal meandering on morphological changes in a meso tidal creek. Estuar. Coast. Shelf Sci. 234, 106635 https://doi.org/10.1016/j.ecss.2020.106635.
van Weerdenburg, R., Pearson, S., van Prooijen, B., Laan, S., Elias, E., Tonnon, P.K., Wang, Z.B., 2021. Field measurements and numerical modelling of wind-driven exchange flows in a tidal inlet system in the Dutch Wadden Sea. Ocean Coast. Manag. 215, 105941 https://doi.org/10.1016/j.ocecoaman.2021.105941.
Willemsen, P.W.J.M., Smits, B.P., Borsje, B.W., Herman, P.M.J., Dijkstra, J.T., Bouma, T. J., Hulscher, S.J.M.H., 2022. Modeling decadal salt marsh development: variability of the salt marsh edge under influence of waves and sediment availability. Water Resour. Res. 58 (1), e2020WR028962 https://doi.org/10.1029/2020WR028962.
Xie, W., He, Q., Wang, X., Guo, L., Zhang, K., 2018a. Role of mudflat-creek sediment exchanges in intertidal sedimentary processes. J. Hydrol. 567, 351–360. https://doi.org/10.1016/j.jhydrol.2018.10.027.
Xie, W., He, Q., Zhang, K., Guo, L., Wang, X., Shen, J., 2018b. Impacts of human modifications and natural variations on short-term morphological changes in estuarine tidal flats. Estuar. Coasts 41 (5), 1253–1267. https://doi.org/10.1007/s12237-017-0352-9.
Xu, Y., Esposito, C.R., Beltrán-Burgos, M., Nepf, H.M., 2022. Competing effects of vegetation density on sedimentation in deltaic marshes. Nat. Commun. 13 (1), Article 1. https://doi.org/10.1038/s41467-022-32270-8.
Yang, S., Ding, P., Chen, S., 2001. Changes in progradation rate of the tidal flats at the mouth of the Changjiang (Yangtze) river, China. Geomorphology 38 (1), 167–180. https://doi.org/10.1016/S0169-555X(00)00079-9.
Yang, S.L., Luo, X., Temmerman, S., Kirwan, M., Bouma, T., Xu, K., Zhang, S., Fan, J., Shi, B., Yang, H., Wang, Y.P., Shi, X., Gao, S., 2020. Role of delta-front erosion in sustaining salt marshes under sea-level rise and fluvial sediment decline. Limnol. Oceanogr. 65 (9), 1990–2009. https://doi.org/10.1002/lno.11432.
Yuan, Y., Li, X., Jiang, J., Xue, L., Craft, C.B., 2020. Distribution of organic carbon storage in different salt-marsh plant communities: a case study at the Yangtze Estuary. Estuar. Coast. Shelf Sci. 243, 106900 https://doi.org/10.1016/j.ecss.2020.106900.
Zhang, Q., Gong, Z., Zhang, C., Townend, I., Jin, C., Li, H., 2016. Velocity and sediment surge: what do we see at times of very shallow water on intertidal mudflats? Cont. Shelf Res. 113, 10–20. https://doi.org/10.1016/j.csr.2015.12.003.
Zhu, Q., 2017. Sediment Dynamics on Intertidal Mudflats: A Study Based on In Situ Measurements and Numerical Modelling. P.hD. thesis,. Delft University of Technology.